A Criterion for Joints Failure

D. Leguillon

Laboratoire de Modélisation en Mécanique, CNRS UMR7607, Université Pierre et marie Curie, 8 rue du Capitaine Scott, 75015 PARIS, France.

ABSTRACT: *The author has proposed a fracture criterion for crack nucleation at stress concentration points (notches, corner points, ...). It involves both strength and toughness of the material and is consistent with the Griffith criterion for a crack. It is employed herein to predict failure of joints. Stress concentration occurs at the interfaces between the joint and the substrates at the end of the joints and it is a privileged site for crack nucleation. Butt and scarf joints are studied with and without thermal residual stresses. The role of a spew fillet in a corner is discussed.*

INTRODUCTION

An important issue in the reliability of joints is the prediction of their load bearing capacity. Failure often occurs at the ends of the joints, at corners in lap joints, at straight edges in butt or scarf joints. They are stress concentrations locations because of the elastic mismatch between the components of the structure and the joint itself which is often much more compliant.
The usual Griffith criterion is inefficient to predict crack initiation at these points. As emphasized by the author in recent papers [1,2], the differential form of the energy criterion must be replaced by an incremental one. This necessary condition for fracture must be completed by the stress criterion. Both are necessary conditions but neither one nor the other is sufficient. They give respectively a lower and an upper bound for admissible crack lengths. The consistency between these two bounds provides a criterion for crack initiation, which coincides with the Griffith one for a pre-existing crack starting to grow. It writes in an Irwin-like form:

$$k \geq k_c \,, \tag{1}$$

where k is the intensity factor of the most significant elastic singular term (characterizing the stress concentration). Its critical value k_c is expressed as

an explicit function of the toughness G_c, the strength r_c and the characteristic exponent λ of the singularity:

$$k_c = \left(\frac{G_c}{K}\right)^{1-\lambda} r_c^{2\lambda-1}. \qquad (2)$$

It involves a scaling coefficient K, which depends on the local geometry of the singular point and on the elastic properties of the neighbouring components. It can be numerically determined using a contour integral [3,4]. The above formula holds for a single real singularity, but it extends to a multiple real singularity, to multiple different real singularities and to complex singularities as met in interface cracks for instance [2].
In a first step the criterion is used to predict failure of butt and scarf epoxy joints in steel and aluminium specimens. Next, a scenario is proposed for failure of spew fillets in lap joints.

BUTT JOINTS

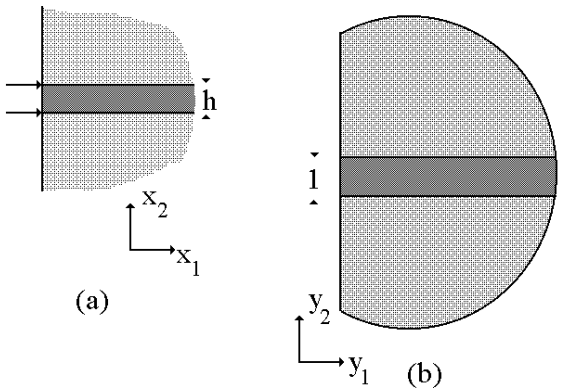

Figure 1: The butt joint, (a) physical domain, (b) stretched domain (the fictitious circular outer boundary is thrown at infinity).

The butt joint (figure 1) made of an epoxy resin (E=3.5 GPa, ν=0.35) between two aluminium (E=69 GPa, ν=0.33) or steel (E=207 GPa, ν=0.30) substrates has been widely analysed by Reedy and Guess [5,6,7] for different joint thickness h. In a first step, the space variables x_i are stretched : $y_i = x_i / h$, then matching conditions between far and near fields (asymptotics in term of the thickness h of the joint) lead to:

$$\underline{U}^h(x_1,x_2)=\underline{U}^h(hy_1,hy_2)=Cte+T\,h\left[\rho\,\underline{t}(\varphi)+\underline{V}(y_1,y_2)\right]+\ldots, \qquad (3)$$

where T is the traction applied to the specimen. Here $\rho\,\underline{t}(\varphi)$ describes the far field, it is the particular solution satisfying $\sigma_{22}=1$ (and vanishing other components) in a homogeneous body (the substrate), $\rho=r/h$ and φ are the polar coordinates. The near field $\underline{V}(y_1,y_2)$ undergoes a singularity (exponent $\lambda<1$) at the end of the interface between the substrate and the epoxy (arrows on figure 1 (a)):

$$\underline{V}(y_1,y_2)=Cte+\kappa\;\rho^{\lambda}\,\underline{u}(\varphi)+\ldots, \qquad (4)$$

where κ is independent of the applied loads. Thus it is computed once for all using a contour integral (the same one used to compute K in (2)). From these two relations, the actual intensity factor k of the singularity reads:

$$k=T\,h^{1-\lambda}\,\kappa\,. \qquad (5)$$

TABLE 1: Comparison with Reedy and Guess experiments, units for k_c are not specified, they are quite entangled and depend on λ.

	λ	λ'	k_c Reedy and Guess	k_c from (2)
Steel	0.70	$1.72 \pm i\,0.59$	11.4 – 15.0	14.3
Aluminium	0.73	$1.73 \pm i\,0.58$	14.0 – 19.6	16.2

The results are summarized in table 1. The toughness G_c (more precisely the opening mode I G_{Ic}) and the strength in traction r_c are taken to be the bulk properties of the epoxy: $G_c=45\ \mathrm{J.m^{-2}}$, $r_c=45\ \mathrm{MPa}$. In this table, the next (complex) exponent λ' of the expansion is exhibited in order to be sure that the first one is well separated from the followings.

THERMAL RESIDUAL STRESSES IN SCARF JOINTS.

The scarf joint can be studied with the same procedure, the singular exponent depends now on the scarf angle γ (figure 2). But, in this section

we are more specifically interested in the role played by the thermal residual stresses in the fracture of these joints as experimentally observed by Kian and Akisanya [8] for different scarf angles $\gamma = 0°,\ 15°$ and $30°$.

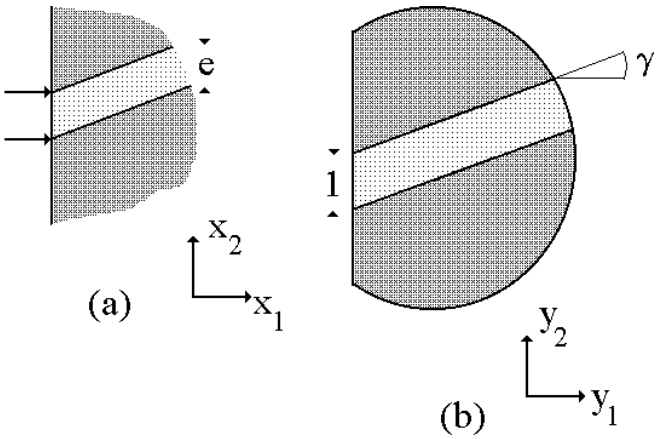

Figure 2: The scarf joint, (a) physical domain, (b) stretched domain.

The solution of the problem splits in two parts: a mechanical and a thermal contribution, the analogous to (3) writes:

$$\underline{U}^h(hy_1, hy_2) = Cte + T\, h\left[\rho\, \underline{t}(\varphi) + \underline{V}(y_1, y_2)\right] + \Theta\, h\left[\rho\, \underline{e}(\varphi) + \underline{W}(y_1, y_2)\right] + \ldots, \quad (6)$$

where Θ is the temperature change and $\rho\, \underline{e}(\varphi)$ the uniform expansion of the aluminium substrate. Using the expansion (4) for both $\underline{V}$ and $\underline{W}$ shows that the intensity factor k splits also in two parts:

$$k = k_m + k_\theta \text{ , with } k_m = T\, h^{1-\lambda}\, \kappa_m \text{ and } k_\theta = \Theta\, h^{1-\lambda}\, \kappa_\theta \text{ .} \quad (7)$$

The main difference with the previous case arises from the computation of the contour integral which holds true only for vanishing body forces and thus cannot be used in presence of thermal residual stresses. A particular local solution of the thermal problem homogeneous to ρ : $\rho\, \underline{w}(\varphi)$, must be removed from $\underline{W}$ to compute κ_θ and compare our prediction with the results of Qian and Akisanya [8].

TABLE 2: Comparison with Qian and Akisanya experiments. Epoxy: $\alpha=5.8\times10^{-5}\,K^{-1}$, $E=3.8\,GPa$, $\nu=0.38$, $r_c=53.3\,MPa$, $G_c=48\,J.m^{-2}$, Al.: $\alpha=2.1\times10^{-5}\,K^{-1}$, $E=70\,GPa$.

Deg, K, mm	λ	k from (7)	k from [8]	k_c from (2)
$\gamma=0, \Theta=100, h=1$	0.72	3.13	3.86	2.45
$\gamma=0, \Theta=140, h=1$	0.72	2.90	3.68	2.45
$\gamma=0, \Theta=100, h=2$	0.72	2.78	3.49	2.45
$\gamma=15, \Theta=100, h=2$	0.71	2.05	2.60	2.23
$\gamma=15, \Theta=140, h=2$	0.71	2.23	2.93	2.23

Results are almost scattered, there are many reasons for that. The first one comes from the material data, r_c for instance can be taken from 45 to 53.3 MPa and G_c from 43 to 48 $J.m^{-2}$. Moreover, as above, the critical values r_c and G_c used in (2) are the bulk properties of the epoxy, whereas (unknown) interface characteristics are required.

The comparison for $\gamma=30°$ is not exhibited. Obviously, traction properties can no longer be invoked alone since the shear component of the stress field plays a growing role as the scarf angle increases. In case of pure shear mode, an analogous analysis based on the shear strength can be carried out. 0therwise, the problems of mode mix remain.

These results can slightly be improved when considering additional terms in the expansions (3) and (6) but of course it leads to more complicated formulas.

FAILURE OF A SPEW FILLET

The last example is dedicated to the study of the bonding of two steel plates ($E=200\,GPa$, $\nu=0.3$) by an epoxy adhesive ($E=2\,GPa$, $\nu=0.36$). Its bearing ability is tested using a three-point bend loading (figure 4).

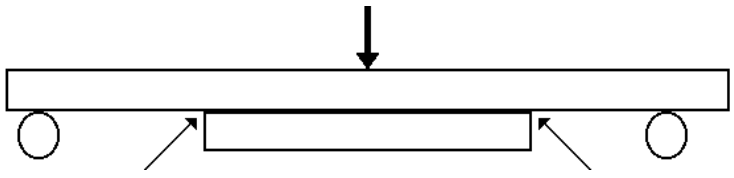

Figure 4: The 3-point bend test.

The weak points are at the ends of the joint (arrows on figure 4) and the stress concentration is governed by the corner singularity $\lambda=0.545$ (the next one $\lambda'=0.907$ is well separated). A spew fillet is added at the end of the joint in order to minimize locally the stress concentration effects (figure 5).

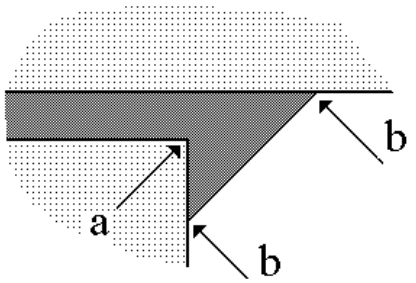

Figure 5: The spew fillet at the end of a bond and the three singular points.

Different crack nucleation scenarios can be considered as shown on figure 6 below.

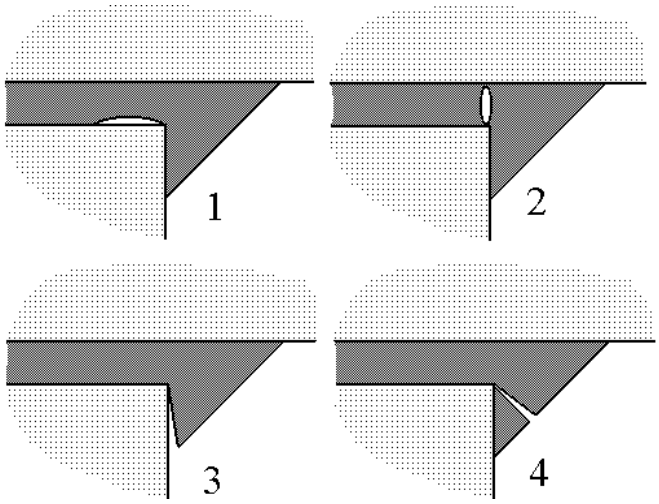

Figure 6: Four crack nucleation scenarios.

The change in potential energy prior to and after nucleation of a micro-crack with length $\delta\ell$ writes at the leading order:

$$\delta W = k^2\, K\, \delta\ell^{2\lambda}\,, \tag{8}$$

where λ is the exponent of the singularity and k is the corresponding intensity factor. The scaling coefficient K was already met in (2). Very few

differences are observed in the value of the scaling coefficient K, the maximum value is achieved in case 1 of figure 6: $K=182\times10^{-5}$ but the deviation does not exceed 2% when analysing the other cases. As a consequence the incremental G is almost the same for the 4 mechanisms. Thus it is the stress state which governs the fracture.
Indeed, the spew fillet reduces the stress concentration effects but does not remove them. Three singular points remain as highlighted by the arrows on figure 5. The most singular is (a) ($\lambda=0.611$, $\lambda'=0.781$) while the two others (b) are very weakly singular ($\lambda=0.985$) due to the angle and to the low stiffness of the epoxy compared to steel.
The singular eigenmodes are normalized in order to have a traction equal to 1 ($\times r^{\lambda-1}$) along the lower horizontal interface. Table 3 summarizes these tractions for the two singular modes in the four cases (figure 6).

TABLE 3: Normalized tractions for the two singular eigenmodes and a combination accounting for the intensity factors.

Case	1	2	3	4
$\lambda=0.611$	1.	-0.39	-1.	-0.06
$\lambda=0.781$	1.	1.09	1.	1.33
Combination	1.00	0.75	0.50	1.00

For very small r, the first singularity is predominant and the case 1 is favoured but for larger r the second term plays a role and the conclusion depends on the ratio of the intensity factors of each term as shown on the bottom line. Another method consists in observing the computed traction along fractures of equal length, this is illustrated in the next figure which shows that the first case is slightly predominant on the fourth one.
A fracture scenario can be derived. In a first step the horizontal interface debonds, then a strong singularity (exponent smaller than ½) develops at the right end of the micro-crack ($\lambda=0.322$, $\lambda'=0.378$). It triggers in a second step the fracture of the remaining ligament of adhesive. Finally the crack can evolve as a delamination crack along the interface or kink into the joint but this is another problem.

CONCLUSION

New examples are proposed in this paper to validate the crack nucleation criterion defined by (1) and (2). They are more specifically dedicated to the

failure of joints. Together with the previous studies (notch in a homogeneous material [1], bimaterial wedge [2]) they incite to trust in the ability of this criterion to predict failure initiation at stress concentration points.

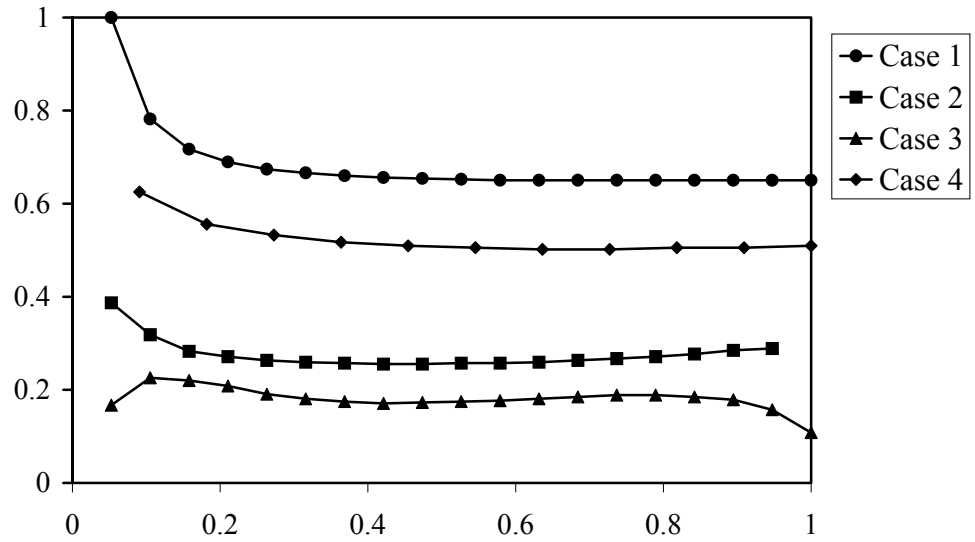

Figure 7: Computed tractions acting prior to the various fracture scenarios vs. the stretched distance $|y|$ to the corner point.

REFERENCES

1. Leguillon, D. (2002), *Eur. J. of Mech. A/Solids*, **21**, 61-72.
2. Leguillon, D., Siruguet, K. (2001) IUTAM symposium on Analytical and Computational Fracture Mechanics of Non-Homogeneous materials, Cardiff, UK.
3. Leguillon, D., Sanchez-Palencia, E. (1987) *Computation of singular solution in elliptic problems and elasticity*, J. Wiley, New York.
4. Labossiere, P.E.W., Dunn, M.L. (1999) *Engng. Fracture Mech.*, **62**, 555-575.
5. Reedy, E.D., Guess T.R. (1993) *Int. J. Solids Structures*, **30**, 21, 2929-2936.
6. Reedy, E.D., Guess T.R. (1997) *Int. J. Fracture*, **88**, 305-314.
7. Reedy, E.D., Guess T.R. (1999) *Int. J. Fracture*, **98**, L3-L8.
8. Qian, Z., Akisanya, A.R. (1998) *Acta. Mater.*, **46**, 14, 4895-4904.